

# Protein–Protein Interactions in Colicin E9 DNase–Immunity Protein Complexes. 2. Cognate and Noncognate Interactions That Span the Millimolar to Femtomolar Affinity Range<sup>†</sup>

Russell Wallis,<sup>‡</sup> Kit-Yi Leung,<sup>‡</sup> Ansgar J. Pommer,<sup>‡</sup> Hortense Videler,<sup>‡</sup> Geoffrey R. Moore,<sup>§</sup> Richard James,<sup>‡</sup> and Colin Kleanthous<sup>\*‡</sup>

*Schools of Biological and Chemical Sciences, University of East Anglia, Norwich NR4 7TJ, U.K.*

*Received May 18, 1995; Revised Manuscript Received August 7, 1995<sup>®</sup>*

**ABSTRACT:** The *in vivo* and *in vitro* cross-binding of the colicin endonuclease-specific immunity proteins toward the DNase domain of colicin E9 is described. *In vivo* cross-protection was tested by toxin plate assays in which bacterial cells overexpressing each immunity (Im2, Im7, Im8, and Im9) were challenged with the ColE9 toxin. Im9, the cognate immunity protein, renders cells completely resistant toward very high concentrations of the toxin (>1 mg/mL), whereas the noncognate immunities display a spectrum of weaker cross-reactivities (<0.01 mg/mL). The order of biological protection in this assay was Im9 ≫ Im2 > Im8, with Im7 providing no colicin E9 resistance. *In vitro* binding between the immunity proteins and the E9 DNase was analyzed by determining the dissociation constants for E9 DNase–Im protein complexes at pH 7.0 in the presence of 200 mM salt and at 25 °C. Stopped-flow fluorescence experiments suggest that both Im2 and Im8 associate with the E9 DNase by a two-step mechanism, in which the rate constants for both the bimolecular association ( $k_1 = \sim 6 \times 10^7 \text{ M}^{-1}\text{s}^{-1}$ ) and the subsequent conformational change ( $k_2 + k_{-2} = 4\text{--}5 \text{ s}^{-1}$ ) are very similar to Im9 binding under the same conditions. Fluorescence chase experiments defined the dissociation rate constants for Im2 and Im8. The estimated values are  $10^6$ - and  $10^8$ -fold, respectively, faster than the off-rate for the Im9 protein. The ratio of the association and dissociation rate constants gives  $K_d$  values of approximately  $10^{-8}$  and  $10^{-6} \text{ M}$  for Im2 and Im8, respectively, whereas the  $K_d$  for Im9 under these conditions is  $10^{-14} \text{ M}$ . The activity of the E9 DNase was also analyzed by an *in vitro* plasmid nicking assay. All three noncognate immunity proteins inhibit the E9 DNase. The  $K_i$ 's for Im2 and Im8 agree closely with the stopped-flow experiments, and the  $K_i$  for Im7 was determined to be  $10^{-4} \text{ M}$ . The order of immunity protein affinity for the E9 DNase (Im9 ≫ Im2 > Im8 > Im7) is the same as that for the *in vivo* toxin protection experiments, implying a correlation between biological specificity and *in vitro* binding. Our results show that the specificity of E9 DNase–Im protein interactions are spread over an affinity range that spans more than 10 orders of magnitude and so offers new opportunities for understanding the basis for specificity in protein–protein interactions.

Protein–protein recognition is fundamental to a myriad of biological processes as diverse as electron transfer, signal transduction, the immune system, transcription activation, and cell motility. Yet compared to the wealth of structural, thermodynamic, and kinetic data that underpin our understanding of the molecular basis for specificity in protein–DNA interactions (Schlief, 1988; Saenger & Heinemann, 1989; Harrison, 1991; Sauer, 1992), relatively little is known about the rules that govern selectivity in protein recognition.

In general, different protein complexes display different affinities depending on the biological role of the complex. Thus, for example, the equilibrium dissociation constants of respiratory electron transfer proteins tend to fall within the millimolar to micromolar range (Erman & Vitello, 1980; Mauk et al., 1982; Pettigrew & Moore, 1987), hormones binding to extracellular receptors and antibodies binding to protein antigens fall in the micromolar to nanomolar range

(Cunningham et al., 1989; Fuh et al., 1992; Kelley & O'Connell 1993; Hawkins et al., 1993), proteinase inhibitors binding to proteinases fall in the nanomolar to femtomolar range (Vincent & Lazdunski, 1972; Empie & Laskowski, 1982; Longstaff et al., 1990), and nuclease inhibitors binding to their target enzymes fall in the picomolar to femtomolar range (Lee et al., 1989; Schreiber & Fersht, 1993). In the preceding paper we address the issue of cognate binding between the DNase domain of colicin E9 with its inhibitor Im9 and find that, similar to other nuclease–inhibitor systems, the dissociation constant for this complex is very low (0.07 fM; Wallis et al., 1995). In the present study, the binding of all members of the endonuclease-specific family of immunity proteins to the DNase domain of colicin E9 has been investigated to address the question of the thermodynamic stability and hence the specificity of these protein–protein interactions.

Colicins are protein toxins made by bacteria to kill other bacteria (Luria & Suit, 1987). The focus of our work has been the E group of endonuclease colicins (61 kDa) which are multifunctional proteins exhibiting three activities: (1) binding to extracellular BtuB receptors (Di Masi et al., 1973), (2) translocation across the bacterial cell membranes, and

<sup>†</sup> This work was supported by the Wellcome Trust and by the U. K. Science and Engineering Research Council.

<sup>\*</sup> Author to whom correspondence should be addressed. Fax: +44 1603 592250. E-mail address: C.Kleanthous@uea.ac.uk.

<sup>‡</sup> School of Biological Sciences.

<sup>§</sup> School of Chemical Sciences.

<sup>®</sup> Abstract published in *Advance ACS Abstracts*, September 15, 1995.

(3) cytoplasmic endonuclease activity (Ohno-Iwashita & Imahori, 1980). Colicin-producing organisms protect themselves by co-expressing a small cytoplasmic inhibitor known as an immunity (Im<sup>1</sup>, 9.5 kDa) protein (Jakes & Zinder, 1974). In the case of the nuclease class of colicins, the immunity protein forms a tight, stoichiometric complex with the C-terminal enzymic domain and so neutralizes its activity in the host. The resulting 71 kDa heterodimeric complex is then released into the medium (Pugsley & Schwartz, 1983).

Four members of the endonuclease class of E group colicins have thus far been identified, E2, E7, E8, and E9. These have almost identical sequences in the regions of the toxin that specify receptor binding and translocation but are only 80% identical in the C-terminal 15 kDa DNase domain (Lau et al., 1992). This variation in sequence is critical for a producing organism since it necessitates the synthesis of an immunity protein specific for each DNase colicin. The corresponding immunity proteins (Im2, Im7, Im8, and Im9) share about 60% sequence identity (Lau et al., 1992).

The traditional view of immunity specificity is one in which each immunity protein protects cells only against its cognate colicin. Indeed, it is an absence of cross-protection that has been used to distinguish one colicin (and its corresponding immunity protein) from another in naturally occurring isolates (Watson et al., 1981; Cooper & James, 1984). What has yet to be addressed in any systematic fashion, however, is whether noncognate interactions are completely excluded or occur with such weak affinity as to offer little protection to the bacterium. This study was therefore designed to compare the *in vivo* and *in vitro* cross-reactivity of both cognate (Im9) and noncognate (Im2, Im7, and Im8) immunity proteins for a single DNase toxin, colicin E9. The data indicate that the affinities of the resulting protein-protein interactions are spread over a very wide range and that this spectrum of affinities is the likely explanation for the biological specificities exhibited by these nuclease inhibitors when overexpressed in bacterial cells.

## EXPERIMENTAL PROCEDURES

**Bacterial Strains and Media.** *Escherichia coli* strains HB101 (Boyer & Roullard-Dussoix, 1969) and JM83 *hsdR*, a restriction-deficient derivative of *E. coli* JM83 (*Ara*<sup>+</sup>, *Lac*<sup>+</sup>, *Pro*, *Thi*, *rpsL*, *φ80DlacZM15*), were used as the host strain for the plasmids. Cultures were grown in Luria-Bertani (LB) broth or on plates of LB agar, supplemented where necessary with ampicillin (100 µg/mL).

**Protein Purifications and Protein Determinations.** Overproduction and purification of Im2, Im7 and Im8 proteins was achieved using a similar strategy to that described previously for Im9 (Wallis et al., 1992a). In each case, the immunity gene was cloned into the expression vector pTrc99A (Pharmacia) and the resulting plasmid introduced into *E. coli* strain JM83 by transformation. Expression was induced by the addition of 1 mM isopropyl β-D-thiogalactoside (IPTG) at an OD<sub>550</sub> of between 0.6–0.8 and the protein purified as described previously (Wallis et al., 1992a). Purification of ColE9 complex and the E9 DNase domain of colicin E9 was carried out as described in Wallis et al.

(1992a, 1994). Protein concentrations were determined as described in Wallis et al. (1995).

**Association and Dissociation Kinetics.** The association and dissociation rate constants for cognate and noncognate complexes were determined by stopped-flow fluorescence and subunit exchange as described in the accompanying paper (Wallis et al., 1995).

**In Vivo Agar Plate Assay.** The biological activities of the immunity proteins were determined using a modified form of the spot test described by Reeves (1965). Five milliliter cultures of *E. coli* JM83 transformed with the vector control (pTrc99A) or vector containing a cloned immunity gene were incubated at 37 °C with shaking in LB medium containing ampicillin (100 µg/mL) until they reached an OD<sub>550</sub> of 0.8 at which point 1 mM IPTG was added and the cultures were incubated for a further 2 h. Samples (200 µL) from each culture were added to 10 mL of molten 0.7% top agar containing 1 mM IPTG, and the mixture was poured onto a single lane of a large LB agar plate (22 cm × 22 cm) which had been separated into five lanes by metal spacers. Once the agar had set 4 µL aliquots of 2-fold serially diluted toxin (typically 12.6–25 ng/mL) were dropped onto each of the lanes, and the plate was incubated overnight at 37 °C. Zones of clearance represent cell death, and the absence of zones indicates biological protection against the action of the toxin. The level of protection conferred by each immunity protein was defined as the concentration of colicin necessary to produce a clear zone of killing using the *in vivo* late assay.

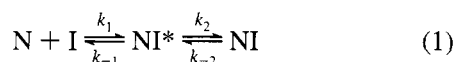
**Preparation of Tritiated pUC18 DNA.** Tritiated pUC18 (<sup>3</sup>H]pUC18) was prepared from 1 L cultures of *E. coli* HB101 transformed with pUC18 (Yanisch-Perron et al., 1985) in M9 media (Sambrook et al., 1989) containing glucose (0.4%), proline (30 µg/mL), tryptophan (30 µg/mL), casein (0.05%), thiamine (0.005%), and ampicillin (60 µg/mL) incubated at 37 °C with shaking. In the late exponential phase (OD<sub>600</sub> = 0.9–1.0) 1 mCi of [*methyl*-<sup>3</sup>H]thymidine (77.2 Ci/mmol) and chloramphenicol (0.2 mg/mL), for plasmid enrichment (Twigg & Sherrat, 1980), were added, and the culture incubated for a further 15 h. The plasmid was purified using cesium chloride density gradient equilibrium sedimentation (two gradients). The typical yield was 400 µg of plasmid DNA (specific activity = 9 nCi/µg).

**In vitro DNase Inhibition Assay.** Inhibition of the E9 DNase by immunity proteins was analyzed by a radioactive plasmid nicking assay based on a method described by Halford et al. (1994). Reactions were carried out at 25 °C in 50 mM Mops buffer, pH 7.0 containing 10 mM MgCl<sub>2</sub>, 0.25 mg/mL bovine serum albumin, 40 µg/mL target DNA (<sup>3</sup>H]pUC18), 1 nM E9 DNase domain, and a range of immunity protein concentrations. Seven samples (5 µL) from each assay (total volume, 35 µL) were taken at timed intervals (over a period of 20–30 min), added to stop-mix (3 µL; containing 100 mM EDTA), and then resolved on an agarose gel (1.2%) to separate the three forms of [<sup>3</sup>H]pUC18: supercoiled, open-circle, and linear. These bands were visualized by ethidium bromide staining and excised from the gel, and their levels of radioactivity were determined by scintillation counting. The rate of supercoil nicking was determined by plotting the log of the percentage supercoil remaining (relative to the starting proportion of supercoiled DNA) in each assay against time, from which pseudo-first-order rates of plasmid nicking could be determined. These

<sup>1</sup> Abbreviations: Im, immunity protein; ColE9, colicin E9; E9 DNase, the isolated 15 kDa endonuclease domain of ColE9; [<sup>3</sup>H]pUC18, pUC18 plasmid which has been biosynthetically radiolabeled with tritiated thymidine; IPTG, isopropyl β-D-thiogalactoside.

values were then plotted as a percentage of control assays, in which no immunity protein had been added, versus the concentration of immunity protein used. These data were then fitted to single ligand binding curves using the ENFITTER programme (Leatherbarrow, Biosoft Publishing Co.).

**Data Analysis.** A two-step reaction model has been proposed by Wallis et al. (1995) for the interaction of Im9 with both ColE9 and its nuclease domain (eq 1) where



nuclease (N) and immunity protein (I) form an encounter complex (NI\*) in a rapid binding step, which then undergoes a slow isomerization to the final folded state (NI).

In this case, the equilibrium dissociation constant is given by the expression

$$K_d = (k_{-1}/k_1)[1 + (k_2/k_{-2})] \quad (2)$$

**Analysis of the Rapid Dilution Experiment on the E9 DNase–Im8 Complex.** On perturbation of the equilibrium position of a two-step reaction, such as eq 1, where the second phase is much slower, the rapid binding step can be treated as independent and

$$k_{\text{obs1}} = k_{-1} + k_1(N + I) \quad (3)$$

where  $k_{\text{obs1}}$  is the apparent association rate constant and  $N$  and  $I$  are the equilibrium concentrations of nuclease and immunity protein for the new condition. For the isomerization step,

$$k_{\text{obs2}} = k_{-2} + k_2/[(1 + k_{-1}/k_1)/(N + I)] \quad (4)$$

Thus,  $k_{\text{obs2}}$  will approach  $k_{-2}$  when  $N + I \ll k_{-1}/k_1$  and  $k_{-2} + k_2$  when  $N + I \gg k_{-1}/k_1$  (Gutfreund, 1972).

## RESULTS

**In Vivo Assays of Immunity Protein Cross-Binding to the ColE9 Toxin.** The biological activities of the four DNase specific immunity proteins toward colicin E9 were examined using a plate assay in which each of the immunity genes encoding Im2, Im7, Im8, and Im9 were overexpressed from the powerful *trc* promoter in *E. coli* JM83 cells. In this way high but similar levels of each immunity protein could be induced by the addition of IPTG. The results from a typical assay are shown in Figure 1. Four main observations can be drawn from the data. (1) In the absence of IPTG, none of the immunity proteins could be observed by SDS-PAGE (Figure 1B), yet the Im9-containing cells still showed complete protection against the highest concentration of the toxin tested ( $>1$  mg/mL; Figure 1C). We interpret this as incomplete repression in the expression system that produces enough protein, of very high affinity [see Wallis et al. (1995)], to protect the cells against the entry of toxin. (2) Assuming that the same level of leakage occurs in the remaining three immunity constructs, then the sensitivity they exhibit (zones evident at  $0.05$   $\mu\text{g/mL}$ ) is typical of naturally occurring isolates producing these noncognate immunity proteins (Figure 1A,1C). (3) On induction with IPTG, high levels of all the immunity proteins are achieved (25–45% of the total cell protein as determined by laser densitometry of SDS–polyacrylamide gels stained with Coomassie blue),

and now intermediate and weak cross-reactivity is observed with Im2 ( $\leq 10$   $\mu\text{g/mL}$ ) and Im8 ( $\leq 0.3$   $\mu\text{g/mL}$ ), respectively (Figure 1A,C). (4) Despite the high levels of Im7 that are produced, no cross-reactivity is observed with this immunity protein.

**Binding Studies of the Noncognate Immunity–E9 DNase Interactions.** The function of each immunity protein is to bind to its cognate colicin thereby neutralizing the bacteriocidal activity within the host cell. *In vitro* studies indicate that the dissociation constant for the cognate colicin E9–Im9 complex at  $25^\circ\text{C}$  is  $9.3 \times 10^{-17}$  M in 50 mM Mops, pH 7.0, corresponding to a free energy change on association of  $-21.9$  kcal  $\text{mol}^{-1}$  (Wallis et al., 1995). With such a high affinity it is not surprising that *E. coli* JM83 cells expressing Im9 show complete biological immunity toward the toxin action of colicin E9. The *in vivo* assay shown in Figure 1 also shows that the non-cognate immunity proteins Im2 and Im8 provide some biological protection for the cells but only when expressed at high levels. The obvious question then is whether this noncognate cross-protection is due to non-cognate protein–protein interactions between the E9 DNase and Im2 and Im8. To investigate this possibility, we determined the dissociation constants for these complexes using rapid binding and exchange kinetics. In all the following binding experiments the isolated 15 kDa E9 DNase domain was used [see Experimental Procedures and Wallis et al., 1994 and 1995].

**Association Kinetics of Noncognate Immunity–E9 DNase Complexes.** Binding between the E9 DNase domain and the noncognate immunity proteins was studied by stopped-flow fluorescence under pseudo-first-order conditions by mixing at least a 4-fold excess of immunity protein with the E9 DNase domain ( $0.35$   $\mu\text{M}$ ) in 50 mM Mops, pH 7.0-containing 200 mM NaCl at  $25^\circ\text{C}$  (see Experimental Procedures and Figure 2). Salt (200 mM) was included in all the experiments to reduce the magnitude of the observed rate constant. Cognate E9 DNase–Im9 binding is known to induce a 15–20% enhancement of the native tryptophan fluorescence of the DNase domain (Wallis et al., 1994,1995). While no change was detected with Im7, a significant fluorescence enhancement was observed on mixing the E9 DNase with either Im2 or Im8 (approximately 50% and 25% of the cognate fluorescence enhancement, respectively). In each case, a two-step binding profile is apparent, in which a fluorescence enhancement is followed by a relatively slow fluorescence quench (Figure 2). The data were fitted to a double-exponential equation. The association profiles are consistent with a two-step binding mechanism similar to that proposed for the cognate E9 DNase–Im9 interaction (eq 1 in Experimental Procedures).

The rate constants  $k_1$  and  $k_{-1}$  for each complex were estimated from the gradient and intercept, respectively, of a plot of the apparent association rate constant ( $k_{\text{obs}}$ ) of the initial fluorescence enhancement against the concentration of immunity protein (inset to Figure 2). Values are shown in Table 1. The intercept for the E9 DNase–Im2 complex was close to zero [ $8.6 (\pm 18)$   $\text{s}^{-1}$ ], and so  $k_{-1}$  could not be determined accurately from the pseudo-first-order plot based on the error limits of the experiment.  $k_{-1}$  for the DNase–Im8 complex was estimated as  $56.8 (\pm 22.2)$   $\text{s}^{-1}$ ; here the dissociation of the encounter complex is significantly faster than the rearrangement step ( $k_2 + k_{-2} = 5.5$   $\text{s}^{-1}$ ).

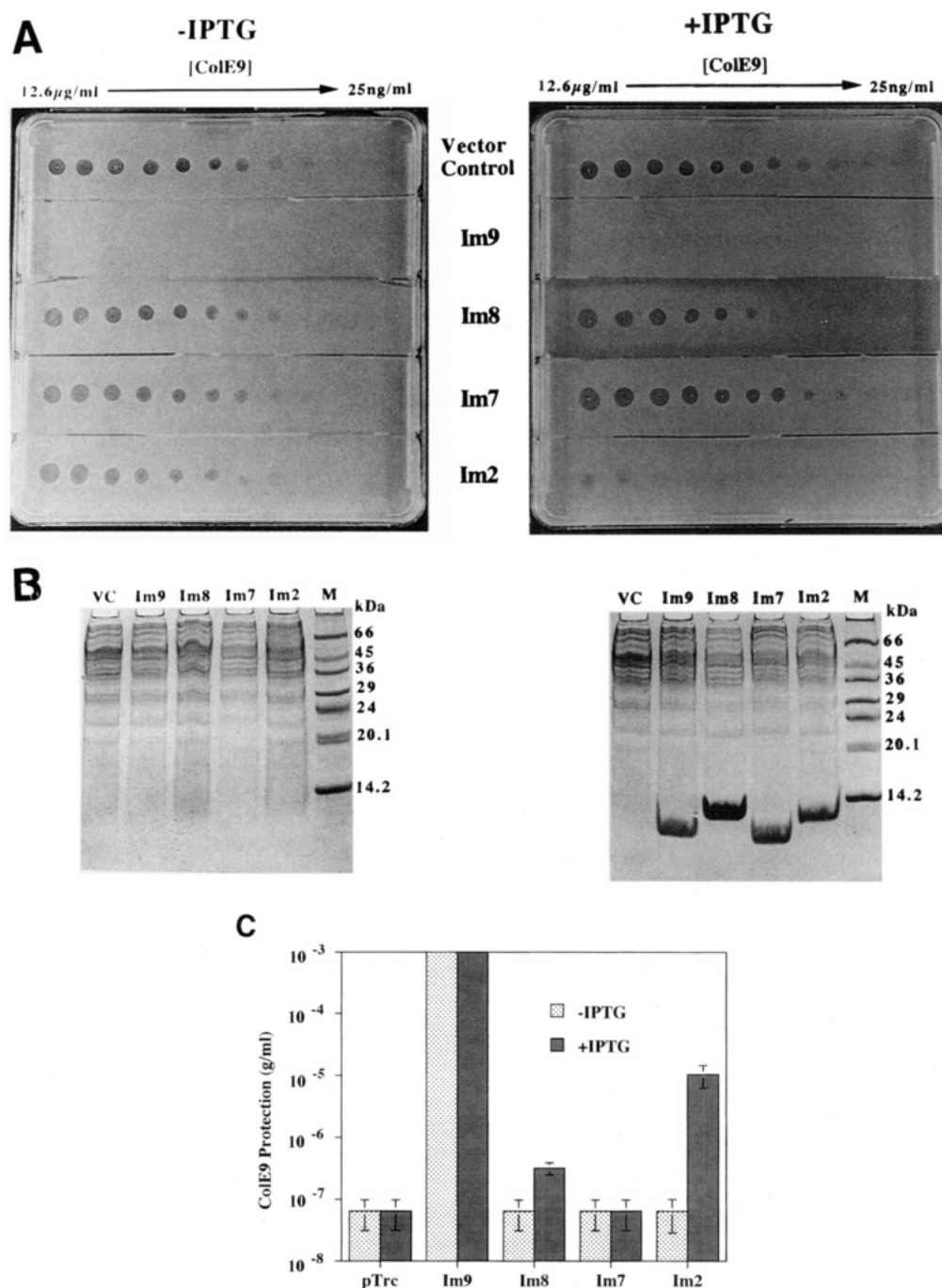


FIGURE 1: (A) *In vivo* agar plate assay demonstrating the biological activities of the E group of colicin nuclease-specific immunity proteins when challenged with ColE9. Each lane was overlaid with a lawn of *E. coli* JM83 cells producing a different colicin-specific immunity protein onto which had been dropped 2-fold serial dilutions (left to right) of purified ColE9 toxin (starting concentration 12.6 μg/mL). Zones of clearance represent cell death, and the absence of zones indicate biological protection against the action of the toxin. Expression of the immunity genes was induced in cultures on the right hand plate by the addition of IPTG (1 mM). (B) Overproduction of immunity proteins monitored by SDS-PAGE. The cells from 1 mL samples of IPTG-induced (right-hand gel) and noninduced cultures (left-hand gel) were boiled in sample buffer and the supernatants loaded onto 16% SDS-polyacrylamide gels in the order shown in the figure. (C) Graphical representation of the *in vivo* biological protection against colicin E9 by nuclease-specific immunity proteins. The level of protection conferred by each immunity protein was defined as the concentration of colicin necessary to produce a clear zone of killing using the *in vivo* plate assay. pTrc is the vector control and represents the basal level of toxin activity against the JM83 cells in this experiment. The data in this histogram were obtained from separate plate experiments in which duplicate lanes were spotted and the average killing activity plotted. The error bars represent the standard errors from these duplicate observations. In separate experiments, cells producing Im9 (±IPTG) were found to be resistant to >1 mg/mL toxin and this is depicted in the figure.

*Dissociation Kinetics of the Noncognate Immunity Protein–DNase Complexes by Stopped-Flow Fluorescence.* Exchange kinetics were used to probe further the dissociation rates of the E9 DNase–Im2 and E9 DNase–Im8 complexes. Radioactive exchange experiments, in which, for example, radiolabeled Im9 is chased from a stoichiometric complex

with the E9 DNase domain by an excess of unlabeled Im9, have been used to measure the overall dissociation rate constant for the cognate complex (Wallis et al., 1995). However, these experiments are only possible when the dissociation rate constant is less than the limiting value of  $3.9 \times 10^{-3} \text{ s}^{-1}$  ( $t_{1/2} > 3 \text{ min}$ ). For the noncognate complexes

Table 1: Kinetic and Thermodynamic Constants for Cognate and Noncognate Immunity Protein–E9 DNase Complexes<sup>a</sup>

| complex                   | $k_1$ (M <sup>-1</sup> s <sup>-1</sup> ) <sup>c</sup> | $k_2 + k_{-2}$ (s <sup>-1</sup> ) <sup>d</sup> | $k_{-1}$ (s <sup>-1</sup> ) | $k_{\text{off}}$ (s <sup>-1</sup> ) | $K_d$ (M)                         | $\Delta G$ (kcal mol <sup>-1</sup> ) |
|---------------------------|---|--|-----------------------------|-------------------------------------|-----------------------------------|--------------------------------------|
| E9 DNase–Im9 <sup>b</sup> | $9.0 (\pm 0.5) \times 10^7$                           | $4.4 (\pm 0.4)$                                | $\ll k_2^e$                 | $2.2 (\pm 0.2) \times 10^{-6}^g$    | $2.4 (\pm 0.4) \times 10^{-14}^i$ | -18.6                                |
| E9 DNase–Im2              | $5.7 (\pm 0.4) \times 10^7$                           | $4.2 (\pm 0.6)$                                | $8.6 (\pm 18.6)^f$          | $0.83 (\pm 0.04)^h$                 | $0.13 - 1.2 \times 10^{-7}^j$     | -9.4 to -10.8                        |
| E9 DNase–Im8              | $6.1 (\pm 0.5) \times 10^7$                           | $5.5 (\pm 0.6)$                                | $56.8 (\pm 22.2)^f$         | $28.2 (\pm 3.0)^h$                  | $0.26 - 0.71 \times 10^{-6}^k$    | -8.4 to -9.0                         |

<sup>a</sup> All experiments were conducted in 50 mM Mops buffer, pH 7.0, containing 200 mM NaCl at 25 °C. <sup>b</sup> Values from Wallis et al. (1995). <sup>c</sup> Rates estimated under pseudo-first-order reaction conditions [Figure 2 and Wallis et al. (1995)]. <sup>d</sup> The first-order quench process which follows the bimolecular collision. <sup>e</sup> Limit set by sequential stopped-flow chase experiments using E9 DNase domain labeled with 5-hydroxytryptophan (Wallis et al., 1995). <sup>f</sup> Values obtained from intercepts of first order rate plots (Figure 2). <sup>g</sup> Values estimated from subunit exchange experiments using tritiated Im9 (Wallis et al., 1995). <sup>h</sup> Values estimated by subunit exchange using stopped flow fluorescence as described in the text and Figure 3. <sup>i</sup> Cognate dissociation constants estimated from the expression  $K_d = k_{\text{off}}/k_1$ . <sup>j</sup> Upper and lower limits for the  $K_d$ , in which the minimum is described by  $k_{\text{off}}/k_1$  and the maximum by eq 1 in Experimental Procedures, where the observed off-rate by exchange =  $k_{-2}$ . <sup>k</sup> Dissociation constant given by eq 1 assuming  $k_2/k_{-2} = 1$ .

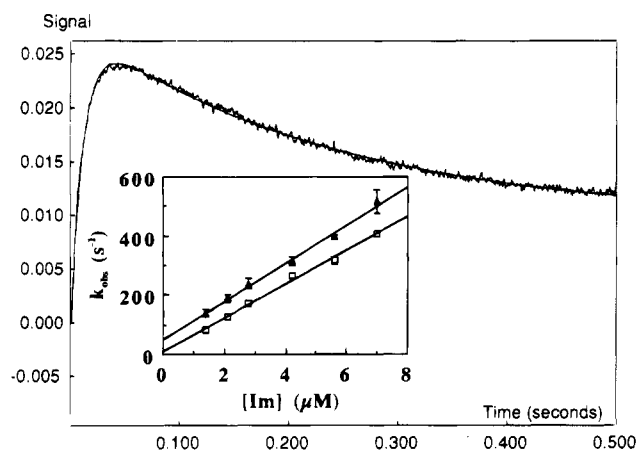


FIGURE 2: Association between the E9 DNase domain (0.35  $\mu\text{M}$ ) and Im2 (1.4  $\mu\text{M}$ ) monitored by stopped flow fluorescence in 50 mM Mops, pH 7.0, containing 200 mM NaCl at 25 °C. The excitation wavelength was 280 nm, and the fluorescence emission was recorded using a 320 nm cutoff filter. The data were fitted to a double-exponential equation. (Inset) Noncognate complex formation monitored under pseudo-first-order reaction conditions using a minimum of a 4-fold excess of Im2 ( $\square$ ) or Im8 ( $\blacktriangle$ ) over the nuclease domain of colicin E9 (0.35  $\mu\text{M}$ ). The association and dissociation rate constants  $k_1$  and  $k_{-1}$  were determined from the gradient and intersect of lines of best fit, respectively. The duplicate data were fitted by linear regression.

it was clear from preliminary experiments that the rate constants were much greater than this limiting value, and so an alternative strategy was employed using stopped-flow fluorescence. The overall fluorescence enhancement of the E9 DNase–Im2 or –Im8 complexes is less than that observed for the cognate complex, and so the dissociation rates were estimated by premixing the E9 DNase and either Im2 or Im8 and then chasing with an equal volume of a 10-fold excess of Im9. Protein concentrations were chosen to ensure that  $\geq 90\%$  of the E9 DNase would be in the bound form.

Figure 3 shows the fluorescence traces resulting from typical chase experiments conducted by stopped-flow. Based on the relative fluorescence intensities of the cognate and non-cognate complexes, the overall fluorescence change observed was found to correspond closely to the estimated value assuming complete exchange for each complex. Chasing the E9 DNase–Im2 complex resulted in a fluorescence enhancement which could be described by an exponential rate equation with a rate constant of  $0.83 (\pm 0.04)$  s<sup>-1</sup> (Figure 3A and Table 1). In this case, it is not clear from the kinetic data which dissociation step ( $k_{-1}$  or  $k_{-2}$ ) is the slower. If  $k_{-2} \ll k_2$ , then  $k_{\text{off}}$ , measured by the chase experiment, approaches  $k_{-2}$  when  $k_{-1} \gg k_2$ . Alternatively,

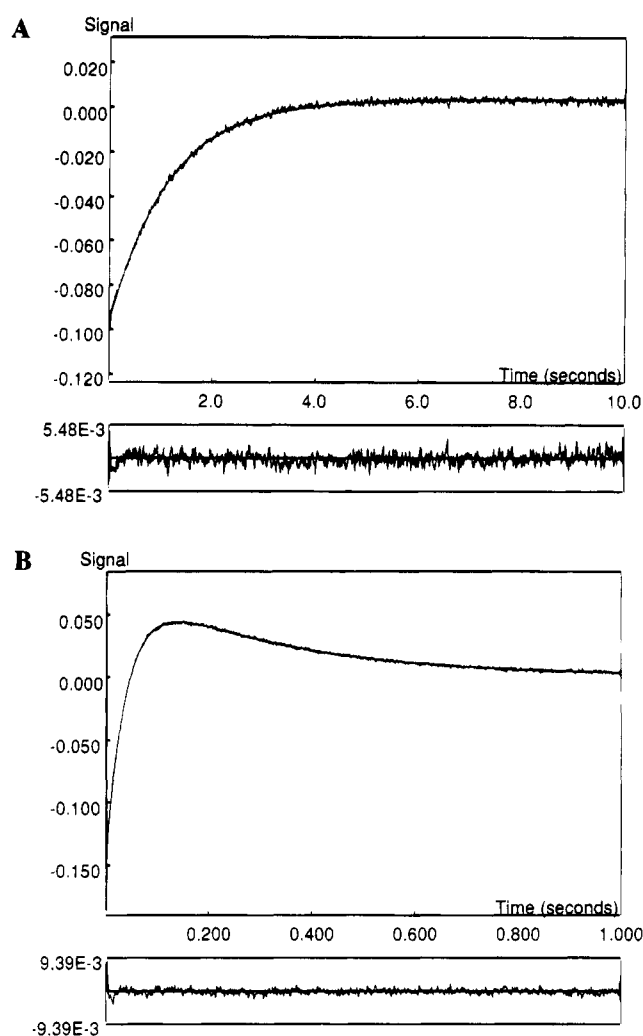


FIGURE 3: Dissociation of the noncognate complexes monitored by stopped-flow fluorescence in 50 mM Mops, pH 7.0, containing 200 mM NaCl at 25 °C. Pre-formed complex between the E9 DNase domain (7  $\mu\text{M}$ ) and either Im2 (A; 21  $\mu\text{M}$ ) or Im8 (B; 21  $\mu\text{M}$ ) was chased with an equal volume of a 10-fold excess of Im9 (210  $\mu\text{M}$ ) and the fluorescence emission ( $> 320$  nm) monitored. The excitation wavelength was 280 nm. The data in panel A were fitted to a single-exponential rate equation, while the data in panel B were fitted to a double-exponential rate equation. The residuals to each of these fits are shown below each figure.

if  $k_{-2} > k_2$ , then the kinetics approach those of a single-step reaction where  $k_{\text{off}} = k_{-1}$ .

An apparent biphasic reaction profile was observed for the E9 DNase–Im8 complex; an initial fluorescence enhancement followed by a fluorescence quench (Figure 3B). Rate constants of  $28.2 (\pm 3.0)$  s<sup>-1</sup> and  $3.4 (\pm 0.2)$  s<sup>-1</sup> were

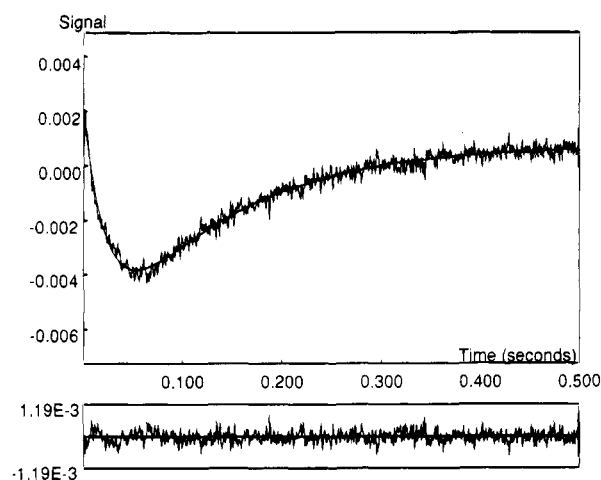


FIGURE 4: Dissociation of the complex between the E9 DNase domain and Im8. Pre-formed complex ( $5.8 \mu\text{M}$ ) was diluted using a 1:10 syringe volume ratio by stopped-flow in 50 mM Mops, pH 7.0, containing 200 mM NaCl at  $25^\circ\text{C}$ . The excitation wavelength was 280 nm, and the fluorescence emission was monitored  $>320$  nm. The data were fitted to a double-exponential rate equation, and the residuals to this fit are shown below the figure.

estimated by fitting the data to a double-exponential rate equation. The rate constant for the initial step is consistent with the previous estimate for  $k_{-1}$  (Figure 2). Since this value is significantly greater than the rate constant of the proposed isomerization step ( $k_2 + k_{-2} = 5.5 \text{ s}^{-1}$ ), this would be consistent with a significant proportion of complex being in the NI\* form at equilibrium. In this case, a biphasic kinetic trace would be expected where the second phase represents dissociation from the NI form. However, the analysis is complicated here since binding between the E9 DNase and Im9, the chase in this experiment, also follows a two-step binding profile where the fluorescence quench represents isomerization of the cognate complex.

In order to further probe the estimate of the dissociation rate constant for the E9 DNase–Im8 interaction, concentration-jump experiments were carried out. Pre-formed complex (at  $5.8 \mu\text{M}$ ; the  $K_d$  estimated by stopped-flow being  $0.2\text{--}0.7 \mu\text{M}$ ) was subjected to rapid dilution using a 1:10 syringe volume ratio in the stopped-flow apparatus, and the resulting fluorescence emission changes were observed. The data in Figure 4 show that dissociation is biphasic; control experiments in which either of the proteins were diluted separately did not yield any time-dependent fluorescence changes (data not shown). There is initially a fluorescence decrease, with a rate constant of  $53.1 \pm (12.4) \text{ s}^{-1}$ , which is followed by a fluorescence enhancement, with a rate constant of  $7.3 \pm (1.0) \text{ s}^{-1}$ . The rate constant for the initial step (eq 3 in Experimental Procedures) is consistent with the previous estimates for  $k_{-1}$  (Table 1), while the second rate is similar to that observed for the proposed complex rearrangement step (eq 4 in Experimental Procedures). These data therefore support the proposed two-step reaction scheme and further suggest that, for the E9 DNase–Im8 complex, a significant proportion is in the NI\* form at equilibrium.

A comparison of the association and dissociation rate constants for E9 DNase cognate and non-cognate complexes is shown in Table 1. For the Im2 complex, since it is unclear which is the rate-determining step for dissociation, upper and lower limits for the  $K_d$  are given in which the minimum is described by  $k_{\text{off}}/k_1$  (where  $k_{\text{off}}$ , the dissociation rate measured

by subunit exchange =  $k_{-1}$ , i.e., where the majority of complex is in the NI\* form at equilibrium) and the maximum by eq 1 in Experimental Procedures, the equation for a two-step reaction mechanism where  $k_{\text{off}} = k_{-2}$ . The dissociation constant for the E9 DNase–Im8 complex was estimated from eq 1 assuming that  $k_2/k_{-2} = 1$ . The data in Table 1 indicate that, under the conditions of these experiments, Im9 binds to its target endonuclease  $10^6$ - and  $10^8$ -fold more tightly than the noncognate immunity proteins, Im2 and Im8, respectively. Hence, the difference in the free energy of binding between cognate and noncognate protein–protein interactions is between 8 and 10 kcal mol $^{-1}$ .

**Inhibition of the E9 DNase Activity by Noncognate Immunity Proteins.** The *in vitro* data up to this point have not addressed the effect of immunity binding on the enzymatic activity of the E9 DNase, and so this was analyzed by a plasmid nicking assay in which [ $^3\text{H}$ ]pUC18 was used as a substrate (Figure 5 and Experimental Procedures). In this assay, the introduction of single- and double-stranded breaks into supercoiled DNA by the nuclease results in relaxation of the plasmid into the open circle and linear conformations. The three plasmid forms were resolved by gel electrophoresis, and the extent of supercoil nicking was quantitated by scintillation counting. This treatment yields pseudo-first-order plots of supercoil nicking activity versus the time of incubation (Figure 5A). From the slopes of these graphs, pseudo-first order rates of supercoil nicking could be determined in the presence and absence of immunity proteins and the ratio of these rates plotted as a function of the immunity protein concentration (Figure 5B). The data for each immunity protein were fitted to single ligand binding curves from which apparent  $K_i$  values for the noncognate complexes could be determined. The fitted values from the curves in Figure 5B are Im2 =  $1.8 (\pm 0.6) \times 10^{-8} \text{ M}$ , Im8 =  $1.3 (\pm 0.5) \times 10^{-6} \text{ M}$ , and Im7 =  $2.4 (\pm 0.6) \times 10^{-4} \text{ M}$ . As expected, cognate binding of Im9 simply results in stoichiometric inhibition of the nuclease activity under the conditions used (Figure 5A). Detailed comparisons between the  $K_d$  and apparent  $K_i$  data are difficult because different conditions were needed for the two experiments (200 mM salt in the stopped-flow experiments and 10 mM  $\text{Mg}^{2+}$  with 0.25 mg/mL BSA in the nicking assay); nevertheless, it is apparent that the noncognate binding of Im2 and Im8 does result in inhibition of the E9 DNase and that the estimated  $K_i$  values derived from this inhibition are similar to the  $K_d$ s determined by fluorescence stopped-flow (Table 1). Im7 was also found to inhibit the E9 DNase but very weakly, and this presumably explains why no evidence for E9 DNase–Im7 association could be obtained by stopped-flow fluorescence experiments.

## DISCUSSION

**In Vitro Affinities Mirror Colicin–Immunity Protein Biological Cross-Reactivity.** The DNase-specific immunity proteins have an important biological role in protecting colicin-producing organisms from the lethal action of the toxin. Since four DNase colicins have now been identified, each bound by a specific immunity protein, this represents an amenable and novel system for investigating protein–protein interaction specificity. One aspect of colicin biology that has hitherto received little attention is the potential for cross-reactivity between a colicin and a noncognate immunity protein. Reports of biological cross-reactivity between

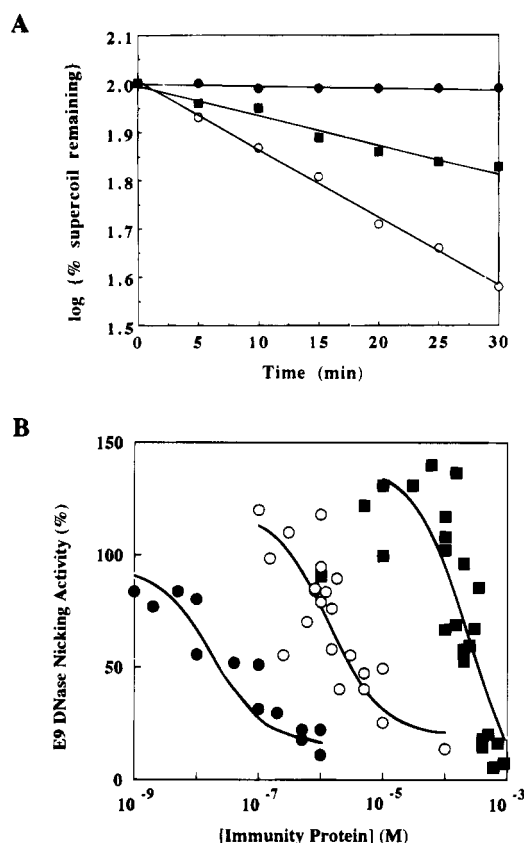


FIGURE 5: Inhibition of E9 DNase activity by cognate and noncognate immunity proteins analyzed by a radioactive plasmid nicking assay. Reactions were carried out at 25 °C in 50 mM MOPS buffer, pH 7.0, containing 10 mM MgCl<sub>2</sub>, 0.25 mg/mL bovine serum albumin, 40  $\mu$ g/mL target DNA ([<sup>3</sup>H]pUC18), 1 nM E9 DNase domain, and a range of immunity protein concentrations. Samples were taken at intervals and resolved by gel electrophoresis to separate the three plasmid forms, the DNA was excised from the gel, and the levels of radioactivity were determined by scintillation counting. (A) Plasmid nicking rates determined in the absence of immunity protein (○), in the presence of a stoichiometric amount of its cognate immunity protein, Im9 (●) and in the presence of 20 nM noncognate immunity protein, Im2 (■). The pseudo-first-order rates were fitted by linear regression. (B). The rate of E9 DNase plasmid supercoil nicking activity in the presence of varying concentrations of Im2 (●), Im7 (■), and Im8 (○) were plotted as a percentage of supercoil nicking in the absence of any immunity protein. Each set of immunity protein inhibition data were then fitted to single ligand binding curves using the ENZFITTER programme (Leatherbarrow, Biosoft Publishing Co.).

nuclease colicins and noncognate immunity proteins have appeared in the literature but have not attempted to evaluate the level of cross-protection or how it might relate to *in vitro* binding. For example, Soong et al. (1992) have observed cross-protection between strains of *E. coli* harboring plasmids expressing ColE2 and ColE8 (and hence their corresponding immunity proteins) when challenged with the ColE7 toxin.

In the present study, we have addressed the issue of biological cross-reactivity using a bacterial overexpression system in which the intracellular levels of all four immunity proteins could be controlled and kept approximately equal (Figure 1B). Using this strategy we are able to show that two of the three noncognate, DNase-specific immunity proteins will provide some element of biological protection toward the action of ColE9, albeit at a lower level than the cognate Im9 protein (Figure 1C). The order of biological protection was therefore Im9  $\gg$  Im2 > Im8, with no protection from Im7. The relative affinities of these im-

munity proteins for the E9 DNase were measured by two methods, stopped-flow fluorescence and plasmid nicking assays (Table 1 and Figure 5), from which the order of tightest to weakest binding was determined to be Im9  $\gg$  Im2 > Im8 > Im7. Therefore, the *in vitro* binding data mirrors the order of biological cross-protection observed for each immunity protein when overexpressed in bacteria. The absence of cross-protection for Im7 is most likely explained by the very weak binding it shows towards the E9 DNase domain (10<sup>-4</sup> M).

**Comparing Cognate and Noncognate Immunity Protein Binding to the E9 DNase.** Stopped-flow fluorescence experiments (Figures 2 and 3) suggest that the mechanism of binding for both cognate and noncognate (Im2 and Im8) immunity proteins to the E9 DNase is the same. Both involve a rapid bimolecular association followed by a slow conformational change, and the rates for each of these processes are very similar (Table 1). Differences are apparent, however, in the magnitude of the initial fluorescence enhancement which is lower for the noncognate complexes. Paradoxically, the subsequent fluorescence quench phase, representing the conformational change, has the same amplitude in both the cognate and the Im2 complexes, suggesting that similar rearrangements are occurring in each case. For the E9 DNase–Im8 complex this amplitude is ~60% of the cognate value, which would be compatible with a significant proportion of the complex being in the NI\* form at equilibrium.

Where the cognate and noncognate complexes differ dramatically is in the rate of their dissociation (Table 1), and it is this which governs the stability of the resulting complexes. This is consistent with other protein complexes where affinities are governed primarily by the dissociation rate constant of the complex (Janin & Chothia, 1990).

**Nuclease Inactivation and Colicin Specificity.** While it is clear that all the DNase-specific immunity proteins will bind to and inhibit the endonuclease domain of colicin E9, what remains unclear is how the enzyme is inhibited and what determines the specificity (and hence binding affinity) of each immunity protein. No structural or mechanistic data are yet available for this class of endonucleases, although both of these areas are currently under investigation. At this point, we can only speculate as to how the enzyme may be inactivated, for example, by steric blocking of the active site as observed with other nuclease inhibitors such as barstar (Guillet et al., 1993; Buckle et al., 1994).

Progress has been made in understanding specificity in this system, both from the point of view of the colicin and the immunity protein. Mutagenesis experiments have identified six amino acids in the central region of the nuclease domain of colicin E9 which confer, at least in part, immunity specificity (Curtis & James, 1991). Gene fusion experiments have identified amino acid residues 16–43 of the 86 amino acid Im9 protein as the region which defines nuclease specificity and mutagenesis data have highlighted position 34 to be an important determinant of this specificity (Wallis et al., 1992b). High-field NMR shows Im9 to be a helical protein with a number of connecting loops in which the specificity, determining region (16–43) spans two of the helices, (I and II), with position 34 displayed from helix II (Osborne et al., 1994). Hence, it seems likely that nuclease recognition by the immunity proteins will involve one or



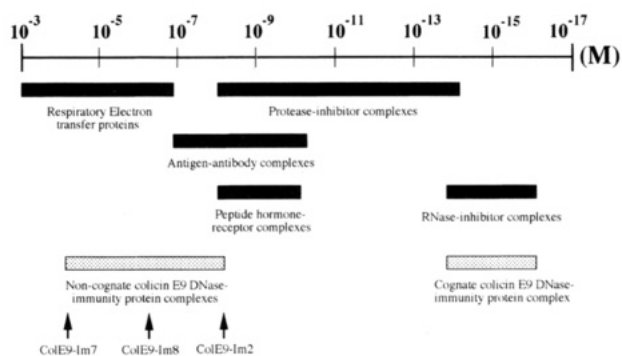


FIGURE 6: Comparison of dissociation constants for E9 DNase–immunity protein complexes with other well studied protein–protein complexes. Colicin data are indicated by hatched boxes and all other complexes with solid boxes. The cognate colicin–immunity protein complex is dependent on the salt concentration, and so a range of  $10^{-14}$ – $10^{-16}$  M is shown. The data for the other complexes were taken from the literature: Respiratory electron transfer proteins (Erman & Vitello, 1980; Mauk et al., 1982; Pettigrew & Moore, 1987); antigen–antibody complexes (Hawkins et al., 1993; Kelley & O’Connell, 1993); peptide hormone–receptor complexes (Cunningham et al., 1989; Fuh et al., 1992); Protease–inhibitor complexes (Vincent & Lazdunski, 1972; Empie & Laskowski, 1982; Longstaff et al., 1990); RNase–inhibitor complexes (Lee et al., 1989; Schreiber & Fersht, 1993).

more residues displayed from helices and these are likely to be involved in differentiating between colicin nuclease enzymes.

**The Specificity of Protein–Protein Interactions and the Colicin System.** Stable protein complexes generally involve large surface areas ( $>600 \text{ \AA}^2$ ) of each protein becoming buried at the interface (Janin & Chothia, 1990; Janin, 1995), and it is likely that similar areas of protein become buried in a colicin DNase–immunity complex. Typically, 10–30 amino acids from each partner form these interacting surfaces, which are highly complementary in shape, charge, and hydrophobicity. Although several different types of protein complexes have been analyzed both at the structural and thermodynamic level, controversy still surrounds the physical basis for the varying stabilities that are observed. For example, the affinity of barstar for the RNase barnase (Schreiber & Fersht, 1993) is approximately five orders of magnitude greater than that of actin for DNase I (Mannherz et al., 1980), yet the surface area that is buried in the latter complex is greater. The surface properties of protein complexes are often compared so as to provide clues as to the reasons behind the observed stability differences; however, no generally applicable rules have yet to emerge from this type of analysis (Janin, 1995).

Dissociation constants for protein complexes span a wide range of affinities, and this is highlighted in Figure 6 where the values for a number of well studied protein–protein interactions are summarized along side the colicin DNase–immunity data from this and the accompanying paper. On the whole, families of protein complexes tend to cluster in particular regions of this affinity scale. Protease inhibitors display a fairly wide range of specificities for target enzymes, and this is due primarily to the identity of the amino acid in the P1 recognition site of the inhibitor (Carrell & Travis, 1985; Bode et al., 1989). Since the immunity proteins are inhibitors of DNases and not proteases, this is not a mechanism of selectivity open to them. Nevertheless, the stabilities of the resulting complexes with the E9 DNase domain span almost the entire range of protein–protein

interaction affinities; from very tight complexes, as observed in RNase–inhibitor systems, to relatively weak interactions, such as are observed in electron transfer complexes.

Assuming that a large surface area is buried in a colicin–immunity complex, how might such varied stabilities be arrived at? One possibility might be that only a limited number of the interacting residues that make up the interface actually contribute substantially to the stability of the complex. This has been observed in a number of studies on tight protein complexes (Novotny et al., 1989; Cunningham & Wells, 1991; Hawkins et al., 1993; Kelley & O’Connell; Clackson & Wells, 1995). Moreover, the work of Clackson and Wells (1995) on human growth hormone binding to its receptor shows that the subset of contact residues that maintain the binding affinity are complementary to each other. They also propose that the peripheral residues of the contact site may be of greater importance in defining the specificity of the interaction by electrostatic or steric repulsion. This is a plausible mechanism for E9 DNase–immunity protein interactions. The postulated specificity determining region of the immunity proteins (residues 16–43) spans two helices (Osborne et al., 1994) and contains many acidic and few basic groups. However, very few of these are conserved between the immunities but rather are distributed differently for each immunity protein.

In conclusion, E9 DNase–immunity protein interactions represent a novel system in the study of specificity in protein–protein interactions. Although sharing  $>60\%$  sequence identity, the immunity proteins provide varying degrees of biological protection toward the action of the ColE9 toxin, and this correlates with the derived dissociation constants for the E9 DNase, which vary from  $10^{-4}$  M for the weakest complex, providing no biological protection, to  $10^{-14}$ – $10^{-16}$  M for the cognate complex, which provides complete biological protection. The specificity of protein–protein interactions is still an elusive and controversial subject, and so the wide range of specificities found in the colicin–immunity protein system offers new opportunities for understanding the underlying principles.

## ACKNOWLEDGMENT

We thank Steve Halford (Bristol) for advice with the plasmid nicking assay, Alan Dawson (Norwich) both for suggesting the stopped-flow dilution experiment and for many stimulating discussions, Clive Bagshaw (Leicester) for help with the stopped-flow fluorescence experiments, Andrew Leech (Norwich) for help with the analysis of the equilibrium binding data, and Ann Reilly and Jill Debbage for their expert technical assistance.

## REFERENCES

- Bode, W., Meyer, E., Jr., & Powers, J. C. (1989) *Biochemistry* 28, 1951–1963.
- Boyer, H. W., & Roulland-Dussoix, D. (1969) *J. Mol. Biol.* 41, 459.
- Buckle, A. M., Schreiber, G., & Fersht, A. R. (1994) *Biochemistry* 33, 8879–8889.
- Carrell, R., & Travis, R. (1985) *Trends. Biochem. Sci.* 10, 20–24.
- Clackson, T., & Wells, J. A. (1995) *Science* 267, 383–386.
- Cooper, P. C., & James, R. (1984) *J. Gen. Microbiol.* 130, 209–215.
- Cunningham, B. C., & Wells, J. A. (1991) *Proc. Natl. Acad. Sci. U.S.A.* 88, 3407–3411.



- Cunningham, B. C., Jhurani, P. N., & Wells, J. A. (1989) *Science* 243, 1330–1336.
- Curtis, M. D., & James, R. (1991) *Mol. Microbiol.* 5, 2727–2733.
- Di Masi, D. R., White, J. C., Schnaitman, C. A., & Bradbeer, C. (1973) *J. Bacteriol.* 115, 506–513.
- Erman, J. E., & Vitello, L. B. (1980) *J. Biol. Chem.* 255, 6224–6227.
- Empie M. W., & Laskowski, M., Jr. (1982) *Biochemistry* 21, 2274–2284.
- Fuh, G., Cunningham, B. C. Fukunaga, R., Nagata, S., Goeddel, D. V., & Wells, J. A. (1992) *Science* 256, 1677–1680.
- Guillet, V., Laphorn, A., Hartley, R. W., & Maugen, Y. (1993) *Structure* 1, 165–176.
- Gutfreund, H. (1972) *Enzymes: Physical Principles*, Wiley, New York.
- Halford, S. E., Taylor, J. B., Vermote, C. L. M., & Vipond, I. B. M. (1994) in *Methods in Molecular Biology* (Kneale, G. G., Ed.), Vol. 30, pp 385–396, Humana Press, Totowa, NJ.
- Harrison, S. C. (1991) *Nature* 353, 715–719.
- Hawkins, R. E., Russell, S. J., Baier, M., & Winter, G. (1993) *J. Mol. Biol.* 234, 958–964.
- Jakes, K. S., & Zinder, N. D. (1974) *Proc. Natl. Acad. Sci. U.S.A.* 71, 3380–3384.
- Janin, J. (1995) *Proteins* 21, 30–39.
- Janin, J., & Chothia, C. (1990) *J. Biol. Chem.* 265, 16027–16030.
- Kelley, R. F., & O'Connell (1993) *Biochemistry* 32, 6828–6835.
- Lau, C. K., Parsons, M., & Uchimura, T. (1992) in *Bacteriocins, Microcins and Lantibiotics* (James, R., Lazdunski, C., & Pattus, F., Eds) pp 353–378, NATO ASI Series H, Springer, Heidelberg.
- Lee, F. S., Shapiro, R., & Vallee, B. L. (1989) *Biochemistry* 28, 225–230.
- Longstaff, C., Campbell A. F., & Fersht A. R. (1990) *Biochemistry* 29, 7339–7347.
- Luria, S. E., & Suit, J. L. (1987) in *Escherichia coli and Salmonella typhimurium, Cellular and Molecular Biology* (Neidhardt, F. C., Ed.) Vol. 2, pp 1615–1624, American Society of Microbiology, Washington, D.C.
- Mannherz, H. G., Goody, R. S. Konrad, M., & Nowak, E. (1980) *Eur. J. Biochem.* 104, 367–379.
- Mauk, M. R., Reid, C. S., & Mauk, A. G. (1982) *Biochemistry* 21, 1843–1846.
- Novotny, J., Bruccoleri, R. E., & Saul, F. A. (1989) *Biochemistry* 28, 4735–4749.
- Ohno-Iwashita, Y., & Imahori, K. (1980) *Biochemistry* 19, 652–659.
- Osborne, M. J., Lian, L.-Y., Wallis, R., Reilly, A., James, R., Kleanthous, C., & Moore, G. R. (1994) *Biochemistry* 33, 12347–12355.
- Pettigrew, G. W., & Moore, G. R. (1987) *Cytochromes c: Biological Aspects* Springer Verlag, Berlin.
- Pugsley, A. P., & Schwartz, M. (1983) *Mol. Gen. Genet.* 190, 366–372.
- Reeves, P. (1965) *Aust. J. Exp. Biol. Med. Sci.* 43, 191–200.
- Saenger, W., & Heinemann, U. (1989) *Protein–Nucleic Acid Interactions*, Macmillan Press, New York.
- Sambrook, J., Fritsch, E. F., & Maniatis, T. (1989) *Molecular Cloning a Laboratory Manual*, second ed., Cold Spring Harbor Laboratory Press, Cold Spring Harbor, NY.
- Sauer, R. T. (1992) *Methods Enzymol.* 208,
- Schlieff, R. (1988) *Science* 41, 12282–12287.
- Schreiber G., & Fersht, A. R. (1993) *Biochemistry* 32, 5145–5150.
- Soong, B.-W., Lu, F.-M., & Chak, K.-F. (1992) *Mol. Gen. Genet.* 233, 177–183.
- Twigg, A. J., & Sherrat, D. J. (1980) *Nature* 238, 216–218.
- Vincent, J.-P., & Lazdunski, M. (1972) *Biochemistry* 11, 2967–2977.
- Wallis, R., Reilly, A., Rowe, A., Moore, G. R., James, R., & Kleanthous, C. (1992a) *Eur. J. Biochem.* 207, 687–695.
- Wallis, R., Moore, G. R., Kleanthous, C., & James, R. (1992b) *Eur. J. Biochem.* 210, 923–930.
- Wallis, R., Reilly, A., Barnes, K., Abell, C., Campbell, D. G., Moore, G. R., James, R., & Kleanthous, C. (1994) *Eur. J. Biochem.* 220, 447–454.
- Wallis, R., Moore, G. R., James, R., & Kleanthous, C. (1995) *Biochemistry* 34, 13743–13750.
- Watson, R. J., Rowsome, W., Tsao, J., & Visentin, L. P. (1981) *J. Bacteriol.* 147, 569–577.
- Yanisch-Perron, C., Vieira, J., & Messing, J. (1985) *Gene* 33, 103–119.